Molybdenum(V) Sites in Xanthine Oxidase and Relevant Analog Complexes: Comparison of Oxygen-17 Hyperfine Coupling

Richard J. Greenwood,[1a] Graham L. Wilson,[1a,b] John R. Pilbrow,[1b] and Anthony G. Wedd*,[1a,c]

Contribution from the Department of Chemistry, La Trobe University, Bundoora, Victoria 3083, Australia, the Department of Physics, Monash University, Clayton, Victoria 3168, Australia, and the School of Chemistry, University of Melbourne, Parkville, Victoria 3052, Australia

Received September 14, 1992

Abstract: Electron paramagnetic resonance at 2-4 and 9 GHz has been used to examine ^{17}O ($I = {}^5/_2$) hyperfine coupling in signals from Mo^V centers in milk xanthine oxidase (Rapid Type 1, Rapid Type 2, Slow) and in the synthetic species $[MoOXL]^-$ and [MoO(XH)L] (X = O, S; LH_2 = *N,N'*-dimethyl-*N,N'*-bis(2-mercaptophenyl)-1,2-diaminoethane) generated in solution. Comparison of the new ^{17}O data with available ^1H, ^{17}O, ^{33}S, and ^{95}Mo information indicates that three ligands can be defined in each of the Mo^V centers derived from active enzyme: Very Rapid, $[Mo^VOS(OR)]$ (OR, product anion); Rapid Type 1 and Type 2, $[Mo^VO(SH)(OH)]$. Formulation of the oxidized resting center as *fac*-$[Mo^{VI}OS(OH)]$ allows derivation of a catalytic cycle consistent with known properties of the enzyme.

Introduction

As a class, the pterin-containing molybdenum enzymes catalyze a variety of two-electron reactions involving net exchange of an oxygen atom between substrate and water.[2-5] A key current question concerns the molecular mechanism of that exchange.

The xanthine oxidase/dehydrogenase systems, in particular, feature a molybdenum cofactor (containing a molybdopterin moiety), two Fe_2S_2 centers, and an FAD center arranged as an internal electron transfer chain[6] with substrate oxidation occurring at the molybdenum site. These enzymes act upon a wide range of substrates but, stoichiometrically, oxidation of a given substrate RH involves formal insertion of an oxygen atom into a CH covalent bond:

$$RH + H_2O \rightarrow ROH + 2H^+ + 2e^-$$

During turnover, the molybdenum site cycles through oxidation states VI, V, and IV. In the absence of X-ray crystallography, EXAFS measurements[7-10] indicate the presence of $[Mo^{VI}OS(SR)_2]$ and $[Mo^{VI}O_2(SR)_{2\text{ or }3}]$ centers, respectively, in the active resting and inactive "desulfo" forms of xanthine oxidase/dehydrogenase. A side chain of the molybdopterin may supply the thiolate ligands as a dithiolene unit.[11] Upon reduction, a single oxo ligand only is detected in both Mo^{IV} forms. The data also suggest that an SH ligand exists in the *active* two-electron reduced state. This presumably results from protonation of the thio ligand present in the Mo^{VI} resting form.

Characteristic Mo^V EPR signals appear in reduced states of the enzymes and have been examined intensively via ^1H, ^{13}C, ^{17}O, ^{33}S, and ^{95}Mo hyperfine coupling interactions.[4,12-15] We have recently compared these data with complementary ^1H, ^{33}S, and ^{95}Mo coupling information from the synthetic species $[MoOXL]^-$ and [MoO(XH)L] (X = O,S; LH_2 = *N,N'*-dimethyl-*N,N'*-bis(2-mercaptophenyl)-1,2-diaminoethane) generated in solution.[15,16] The comparison consolidates assignment of the following partial structures to the centers responsible for the EPR signals:

Very Rapid:	$[Mo^VOS]$
Rapid Type 1:	$[Mo^VO(SH)]$
Rapid Type 2:	$[Mo^VO(SH)(OH)]$
Slow:	$[Mo^VO(OH)]$

Hille's single turnover experiments[17,18] are an important contribution to an understanding of the reaction mechanism. They show that (i) the oxygen atom transferred to the substrate originates from the enzyme and not directly from solvent H_2O, (ii) *only* the Very Rapid signal is seen under substrate limiting conditions and is formed via one-electron oxidation of a Mo^{IV} species, and (iii) the Rapid Type 1 signal appears *only* in the presence of excess substrate.

Both the Very Rapid and Rapid Type 1 centers have been implicated in the main catalytic pathway,[13,15,19] but there are contrary views.[18] Product OR bound as a molybdenum ligand (structure I for uric acid anion formed from substrate xanthine RH by attack at the C_8H bond) has been suggested for both these

(1) (a) La Trobe University. (b) Monash University. (c) University of Melbourne.
(2) Coughlan, M. P., Ed. *Molybdenum and Molybdenum-containing Enzymes*; Pergamon Press: Oxford, New York, 1980.
(3) Spiro, T. G., Ed. *Molybdenum Enzymes*; John Wiley, New York, 1985.
(4) Bray, R. C. *Q. Rev. Biophys.* **1988**, *21*, 2990.
(5) Holm, R. *Coord. Chem. Rev.* **1990**, *110*, 183.
(6) An intriguing recent paper reports that the Fe_2S_2 centers are not essential for catalytic turnover in xanthine dehydrogenase from *Drosophila Melanogaster* (Hughes, R. K.; Bennett, B.; Bray, R. *Biochemistry* **1992**, *31*, 3073).
(7) Cramer, S. P. Adv. *Inorg. Bioinorg. Mech.* **1983**, *2*, 259.
(8) Hille, R.; George, G. N.; Eidness, M. K.; Cramer, S. P. *Inorg. Chem.* **1989**, *28*, 4018.
(9) Turner, N. A.; Bray, R. C.; Diakin, G. P. *Biochem. J.* **1989**, *260*, 563.
(10) George, G. N.; Cleland, W. E., Jr.; Enemark, J. H.; Smith, B. E.; Kipke, C. A.; Roberts, S. A.; Cramer, S. P. *J. Am. Chem. Soc.* **1990**, *112*, 2541.
(11) Rajagopalan, K. V.; Johnson, J. L. *J. Biol. Chem.* **1992**, *267*, 10199 and references therein.
(12) (a) Bray, R. C.; Gutteridge, S. *Biochemistry* **1982**, *21*, 5992. (b) Tanner, S. J.; Bray, R. C.; Bergmann, F. *Biochem. Soc. Trans.* **1978**, *6*, 1328.
(13) George, G. N.; Bray, R. C. *Biochem. Soc. Trans.* **1987**, *13*, 570.
(14) George, G. N.; Bray, R. C. *Biochemistry* **1988**, *27*, 3603.
(15) Wilson, G. J.; Greenwood, R. J.; Pilbrow, J. R.; Spence, J. T.; Wedd, A. G. *J. Am. Chem. Soc.* **1991**, *113*, 6803.
(16) Dowerah, D.; Spence, J. T.; Singh, R.; Wedd, A. G.; Wilson, G. L.; Farchione, F.; Enemark, J. H.; Kristofzski, J.; Bruck, M. *J. Am. Chem. Soc.* **1987**, *109*, 5655.
(17) Hille, R.; Sprecher, H. *J. Biol. Chem.* **1987**, *262*, 10914.
(18) McWhirter, R. B.; Hille, R. *J. Biol. Chem.* **1991**, *266*, 23724.
(19) Bray, R. C. *Adv. Enzymol. Relat. Areas Mol. Biol.* **1980**, *51*, 107.

0002-7863/93/1515-5385$04.00/0

Table I. Hyperfine Coupling ($\times 10^{-4}$ cm^{-1}) to ^{17}O in Xanthine Oxidase and Analog Systems

	g[b]				A[b]					
system[a]	x	y	z	av	x	y	z	α_{xy}[d]	av	ref
$[MoO(SPh)_4]^-$	1.979	1.979	2.017	1.990	2.86	2.86	0.64		2.12	27a
[MoO(SH)L]	1.952	1.960	2.016	1.976	2.9(2)	3.0(2)	0.75(2)		2.2(3)	
$[MoOSL]^-$	1.889	1.934	2.017	1.946	2.2(1)	3.1(3)	1.4(1)		2.2(3)	
[MoO(OH)L]	1.944	1.947	1.981	1.957	2.8(5)	2.8(5)	1.1(5)		2.2(4)[c]	
					13(2)	3(1)	7(1)		7.6(2)[c]	
$[MoO_2L]^-$	1.987	1.916	1.811	1.904	3.5(2)	12.9(2)	6.3(2)		7.7(4)[g]	
very rapid: xanthine	1.9494	1.9550	2.0252	1.9571	12.7	12.8	12.4		12.6	29
rapid type 1: formamide	1.9663	1.9712	1.9904	1.9760	14.7	2.8	1.4	35	6.3	30
rapid type 1: 1-methylxanthine	1.965	1.969	1.989	1.974	14.7(1)	2.8(1)	1.9(1)	38(5)	6.5(2)[g]	
rapid type 2: borate	1.967	1.968	1.990	1.973	2.8(3)[e]	11.6(2)[e]	1.8(3)		5.4(5)[g]	
slow: aquo	1.954	1.966	1.971	1.963	10(2)					
inhibited: formaldehyde	1.9513	1.9772	1.9914	1.932	1.2	2.9	0.6[f]			12
					1.5	1.1	1.1[f]			

[a] For the enzyme spectra, the substrate inducing the signal is listed. [b] g values for the analog compounds taken from refs 15 and 27a. Other parameters are taken from the references listed. Errors in **g**: 1 in the third decimal. Errors in **A**: the estimates in parentheses were obtained by varying the parameters one at a time to the point at which discernible differences appeared. [c] Determined from liquid solution measurements at −42 °C and 2.3 GHz. [d] Angle of coincidence between g_x and A_x and between g_y and A_y. [e] Tentative assignments: these may be switched (see text). [f] The combination of couplings given is arbitrary: see ref 12. [g] Calculated assuming the signs of the components are all the same.

centers,[15,16,20] although ^{13}C coupling from the xanthine C_8 atom under attack is seen for the Very Rapid signal only.[12b]

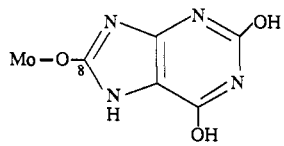

I: Mo—OR

This paper compares the anisotropic ^{17}O hyperfine coupling observed for the xanthine oxidase EPR signals with those of the species $[MoOXL]^-$ and [MoO(XH)L] (X = O, S) to supplement the ^{1}H, ^{33}S, and ^{95}Mo data obtained previously.[15,16] The results allow definition of three molybdenum ligand positions for the Very Rapid, Rapid Type 1, and Rapid Type 2 centers. The spectacular differences in the magnitude and anisotropy of the ^{17}O coupling seen in the Very Rapid and Rapid Type 1 signals (Table I) are addressed. A molecular mechanism of reaction is derived. A generalized oxygen atom transfer mechanism has been formulated for the molybdenum hydroxylase enzymes.[5,22] For xanthine oxidase with its $[Mo^{VI}OS]$ resting center, this seems to imply the existence of a transient deoxomolybdenum(IV) intermediate. Formulation of the resting center as *fac*-$[Mo^{VI}OS(OH)]$ eliminates the need for such an intermediate.

Experimental Section

All manipulations of molybdenum species in solution were performed under purified argon or dinitrogen gas using standard Schlenck and gas-tight syringe techniques.

Materials. Xanthine oxidase was isolated as described previously.[15] Solvents were dried and purified as described previously.[15] Alumina (Merck) was activated by drying at 200 °C at 0.05 mmHg pressure for 16 h. α-$(Bu^n_4N)_4[Mo_8O_{26}]$ (^{98}Mo: 98.75 atom %) and LH_2 were prepared as described previously.[15,16] H_2O (^{17}O: 56.4 and 51.5 atom %) was obtained from the Monanto Research Corp. MoO_2L labeled with both ^{98}Mo and ^{17}O was prepared as follows: MeCN, MeOH, and CH_2Cl_2 were dried further by stirring overnight over activated alumina. H_2O (110 μL; 6.1 mmol) was added to a solution of α-$(Bu_4N)_4[Mo_8O_{26}]$ (81.2 mg; 0.30 mmol) in MeCN (1.5 cm^3). The solution was stirred at room temperature for 20 h. The substitution process was repeated on the residue providing a calculated concentration of ^{17}O of 55.3 atom % assuming 100% exchange efficiency. An infrared spectrum revealed that the characteristic $\nu(Mo^{16}O)$ absorptions in the 950-600 cm^{-1} region had broadened and shifted to lower energy. The pale yellow residue (70 mg) was added to MeOH (3.2 cm^3) containing added $H_2{}^{17}O$ (50 μL; 2.8 mmol). Addition of LH_2 (113 mg; 0.371 mmol) in CH_2Cl_2 (0.5 cm^3) gave a clear solution which darkened immediately. An orange precipitate formed progressively at 0 °C over 0.5 h. The product was filtered, washed with MeOH, dried under vacuum, and stored under dinitrogen (yield: 77.6 mg, 0.179 mmol; 69%).

EPR Samples. Xanthine oxidase (40–60 mg cm^{-3}) in bicine buffer (50 mM; pH 8.2) as frozen beads was freeze-dried for 4 h at a pressure of 10^{-3} mmHg. The residue was dissolved in H_2O (51.5 atom % ^{17}O) and allowed to stand under argon for 3 h before preparation of the EPR samples. The 1-methylxanthine Rapid Type 1, borate Rapid Type 2, and aquo Slow signals were generated by the methods of Bray.[23-26] In each case, the ^{16}O spectra were in satisfactory agreement with the published spectra. Samples of $[MoO_2L]^-$, [MoO(OH)L], $[MoOSL]^-$, and [MoO(SH)L] were prepared from the labeled $[MoO_2L]$ using methods and solvents described previously.[15] However, all solvent systms were predried over alumina and then made approximately 50 mM in $H_2{}^{17}O$ in an attempt to suppress loss of ^{17}O label.

EPR Measurements. Varian E-9 and E-12 spectrometers operating at X-band (ca. 91 GHz) and using E231 cavities were employed. The low-frequency measurements were carried out by using a home-built 1-4 GHz tuneable reference arm bridge attached to the E-12 spectrometer. Home-built loop gap resonators tuned at 3.6 GHz were manufactured from Macor ceramic and subsequently silver plated. Frequencies were measured with an EIP 548-A frequency counter. Magnetic field calibration was obtained via the proton resonance of water. Spectra were recorded on an LSI 11/23 microcomputer coupled to a VAX 11/780 computer.

EPR spectra of glasses at 77 or 130 K are provided in Figures 1–6 and were acquired at 9.1 and 3.6 GHz and, when indicated, at 2.3 GHz. Simulations employed the EPR50F program[27,28] which provides for consideration of nuclear hyperfine coupling to the nuclei of up to five different ligand atoms. It also allows for non-coincident metal ion **g** and **A** principal axes for symmetries as low as monoclinic. In practice, it is possible to test for non-coincidence about any one of the three principal **g** axes. While the non-coincidence angles thus obtained are not easily determined to high precision, a matter related to the resolution and line widths observed, nevertheless, in the examples given in this paper, such low symmetry would be expected in any case. It proves easier to estimate the non-coincidence angles at X-band but not at the lower microwave frequencies also used in the experiments. Where multiple frequency data are reported, it has been our goal to report simulations at all frequencies using a single parameter set of g values, A values, line width parameters, etc.

(20) Wilson, G. L.; Kony, M.; Tiekink, E. R.; Pilbrow, J. R.; Spence, J. T.; Wedd, A. G. *J. Am. Chem. Soc.* **1988**, *110*, 6923.
(21) Gutteridge, S.; Tanner, S.; Bray, R. C. *Biochem. J.* **1978**, *175*, 869.
(22) Holm, R. *Chem. Rev.* **1987**, *87*, 1401.
(23) Gutteridge, S.; Malthouse, J. P. G.; Bray, R. C. *J. Inorg. Biochem.* **1979**, *11*, 355.
(24) Malthouse, J. P. G.; Williams, J. W.; Bray, R. C. *Biochem. J.* **1981**, *197*, 421.
(25) Malthouse, J. P. G.; Gutteridge, S.; Bray, R. C. *Biochem. J.* **1980**, *185*, 767.
(26) Lowe, D.; Barber, M. J.; Pawlik, R. T.; Bray, R. C. *Biochem. J.* **1976**, *155*, 81.
(27) Pilbrow, J. R. *J. Magn. Reson.* **1984**, *58*, 186.
(28) (a) Hanson, G. R.; Wilson, G. L.; Bailey, T. D.; Pilbrow, J. R.; Wedd, A. G. *J. Am. Chem. Soc.* **1987**, *109*, 2609. (b) Wilson, G. L., Ph.D. Thesis, La Trobe University, 1988. (c) Greenwood, R. J., M.Sc. Thesis, La Trobe University, 1991.

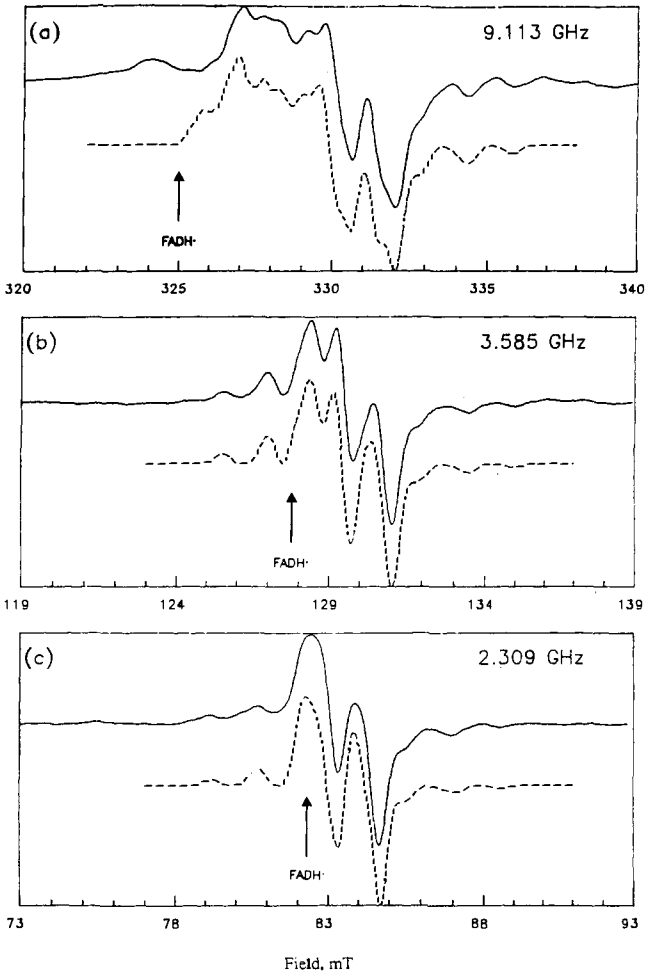

Figure 1. Experimental (solid line) and simulated (dashed line) spectra of the 1-methylxanthine Rapid Type 1 Mo^V EPR signal of xanthine oxidase (^{17}O, $I = {}^5/_2$, 50 atom %), 150 K. The arrow indicates the expected resonance position of contaminating FADH radical from the flavin cofactor.

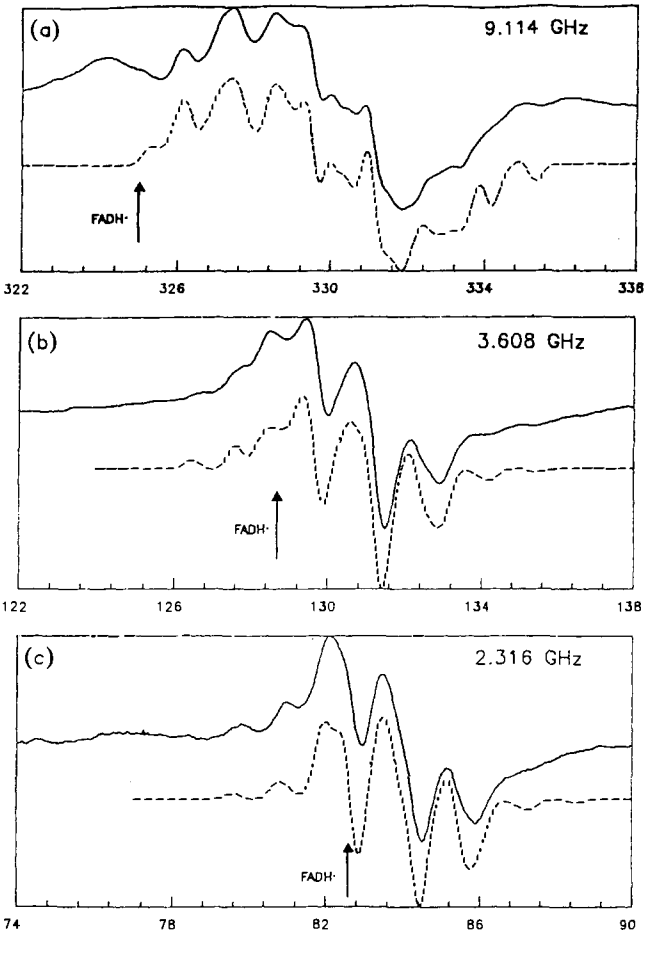

Figure 2. Experimental and simulated spectra of the borate Rapid Type 2 Mo^V EPR signal of xanthine oxidase (^{17}O, $I = {}^5/_2$, 50 atom %), 150 K.

The **g** and **A**(^1H) tensors have been listed previously,[15] and the ^{17}O coupling parameters listed in Table I are those which provide optimal simulations at all frequencies used (Figures 1–6). Metal-centered coordinate systems for the analog compounds are defined in Figure 7.

Results

A natural abundance of 0.037 atom % means that detection of ^{17}O ($I = {}^5/_2$) coupling in the EPR spectra of $Mo^V(4d^1)$ species requires isotope enrichment. Water enriched in ^{17}O up to about 56 atom % is available.

Enzyme Spectra. The detection at X- and Q-band frequencies of strong isotropic coupling from a single oxygen atom in the Very Rapid signal is clear-cut,[29] and so that signal was not included in the present work at lower frequencies. The 1-methylxanthine Rapid Type 1 spectrum seen at 9.1 GHz (Figure 1) is very similar to the purine and formamide signals reported previously.[23-26,29] The low spectral spread at the lower frequencies (3.6 and 2.3 GHz) leads to improved resolution of ^{17}O hyperfine structure in both the high and low field portions of the ^{16}O features. This structure is field independent (Figure 1) and is associated only with the single high-field g value (g_x, 1.9646). The low frequency spectra are less affected by non-coincidence between **g** and **A**.[15] After successful simulation of the low-frequency spectra, the X-band spectrum was simulated by introduction of non-coincidence between the axes of **g** and **A**(^{17}O) while holding all other parameters constant. The single set of parameters listed in Table I provides excellent simulations at each of the three frequencies (Figure 1).

^{17}O coupling in the borate Rapid Type 2 spectrum at 9.1 GHz (Figure 2) causes broadening and loss of resolution but little clear additional structure. There is a significant proportion of FADH signal apparent in the present sample. At the lower frequencies, ^{17}O structure is revealed clearly (compare with the ^{16}O spectrum in Figure 2a of ref 15). While the simulations in this difficult case are not as successful as those described above, they again indicate that a single O nucleus is coupled anisotropically. The complex splitting patterns arising from two near equivalent protons and at least one O ligand (at least 18 lines per direction) make definitive assignments very difficult. In particular, given that **g** is nearly axial, the strongest coupling may be associated with g_y rather than with g_x and the simulations were somewhat improved with that assumption. The presence of a second more weakly coupled oxygen, such as that observed for a terminal oxo group (*vide infra*), cannot be discounted from the present work.

Two coupled ^{17}O atoms have been proposed previously via difference spectral techniques applied to samples of different isotope enrichment.[12a] Unfortunately, neither the anisotropy nor the magnitude of the coupling could be deduced except to estimate an average ^{17}O coupling constant of about 1 mT for the more strongly coupled atom. The present work provides more information about the magnitude and anisotropy of that coupling (Table I). As stated previously,[12] full interpretations may require doubly labeled water ($^2H_2{}^{17}O$) which is not currently available.

The aquo Slow signal[12] also shows additional shoulders assignable to ^{17}O coupling (spectra not shown). While structure

(29) Gutteridge, S.; Bray, R. C. *Biochem. J.* **1980**, *189*, 615.
(30) Morpeth, F. F.; George, G. N.; Bray, R. C. *Biochem. J.* **1984**, *220*, 235.

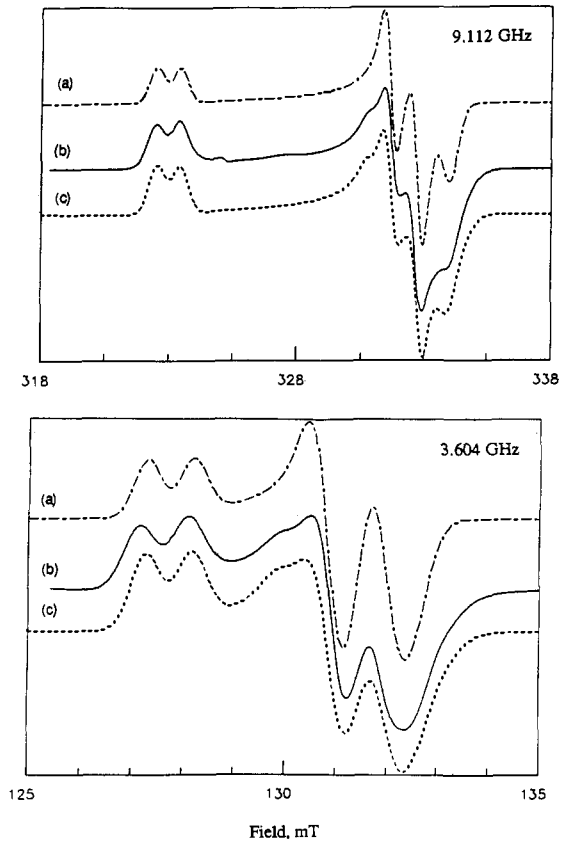

Figure 3. Experimental and simulated spectra of [MoO(SH)L] (^{98}Mo, I = 0, 98.75 atom %) in 1:1 thf:MeCN, $Bu^n_4BF_4$ (0.1 M), and H_2O (2 M); 130 K: (a) ^{16}O, I = 0, 100 atom %; (b) ^{17}O, $I = {}^5/_2$, 52 atom %; (c) simulation of (b).

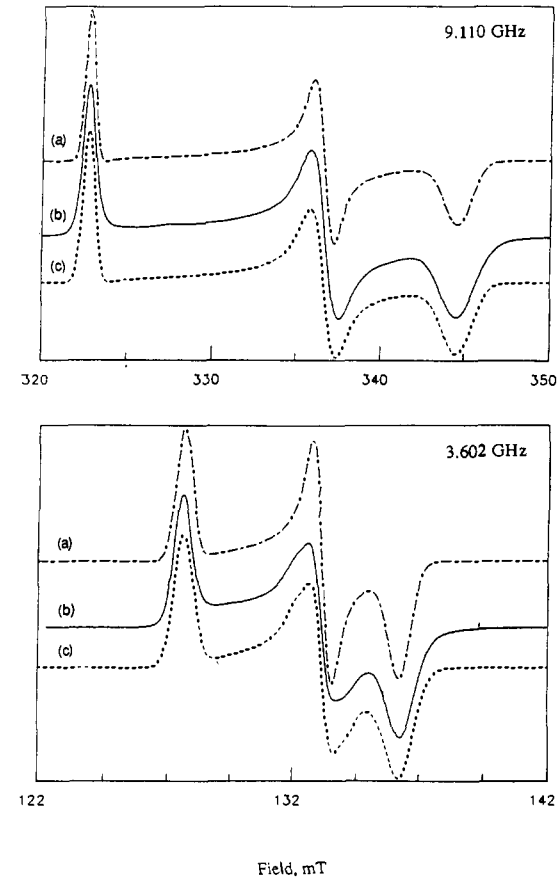

Figure 4. Experimental and simulated spectra of [MoOSL]$^-$ (^{98}Mo, I = 0, 98.75 atom %) in 1:1 thf:MeCN, $Bu^n_4BF_4$ (0.1 M), and H_2O (2 M); 130 K: (a) ^{16}O, I = 0, 100 atom %; (b) ^{17}O, $I = {}^5/_2$, 52 atom %; (c) simulation of (b).

is apparent at low and high field at the lower frequencies, the resolution was inadequate to justify detailed simulation. The structure was associated with g_x (Table I), and comparison with the above cases again indicates the presence of a single anisotropically coupled O nucleus. However, this assignment remains tentative as other possibilities cannot be discounted.

Analog Compound Spectra. While a number of dioxomolybdenum(VI) species undergo ^{17}O exchange with H_2O directly,[31,32] [MoO_2L] does not. Presumably, this property is related to the steric barrier imposed by ligand L[15,33] and which allows convenient detection of the Mo^V species examined here. Interestingly, oxygen exchange is slow in the Mo^{VI} resting form of xanthine oxidase ($t_{1/2} \sim 1$ h) but about 30 times faster in reduced enzyme.[17,29] Slow exchange into [Mo^VO_2L]$^-$ and [Mo^VOSL]$^-$ was observed at room temperature in the present work, but not at the lower temperatures (<–40 °C) at which the conjugate acid forms *cis*-[MoO(OH)L] and *cis*-[MoO(SH)L] must be generated. Consequently, the ^{17}O label was introduced into the precursor [Mo_8O_{26}]$^{4-}$ ion before synthesis of [MoO_2L]. As a further precaution, all predried solvents used were spiked with enriched H_2O (about 50 mM). The nonmagnetic ^{98}Mo isotope at 98.75 atom % was used to eliminate the complications of the ^{95,97}Mo coupling observed at natural abundance.[15]

[MoO(SH)L]. All features are broadened by ^{17}O coupling with a shoulder apparent on the low-field side of the y, x components (Figure 3). Simulation was straightforward and satisfactory and A(^{17}O) is axial within experimental error.

[MoOSL]$^-$. All features are broadened (Figure 4). No angles were included in the simulations because of the lack of resolution of the hyperfine structure. In addition, note that the coupling in the z direction is weak and this plus the large line width of the x component at high field means that the simulation is relatively insensitive to misalignment of **g** and A(^{17}O) in the xz plane. Consequently, the orientation of A(^{17}O) is uncertain.

[MoO(OH)L]. A preliminary communication[20] presented a liquid solution spectrum measured at –42 °C and 2.4 GHz with a ^{17}O content of 30 atom %. Three of the four possible isotopomers (^{16}O^{16}O^{1}H; ^{16}O^{17}O^{1}H; ^{17}O^{16}O^{1}H) were observed directly via characteristic ^{17}O and ^{1}H coupling (Figure 2 of ref 20). An increase in the level of ^{17}O enrichment to 40 atom % was achieved in the present work[34] providing the isotopomers in relative concentration of 9:6:6:4. However, the ^{17}O^{17}O^{1}H species again could not be detected directly, presumably due to the low relative intensity of its dispersed 72-line spectrum. The quality of the new simulation (cf. Figure 2 of ref 20) confirms coupling to two inequivalent oxygen atoms with average coupling constants of 2.2(4) and 7.6(2) × 10^{-4} cm^{-1}, assigned to the oxo and hydroxo ligands, respectively.

The frozen solution spectrum exhibits broadening of all components and additional features at low and high fields (Figure 5). The overall lack of resolution is disappointing, however. The approach to this difficult simulation assumed an axial ^{17}O tensor for the oxo ligand similar to that observed for [MoO(SH)L]. The ^{16}O^{16}O^{1}H and ^{17}O^{16}O^{1}H spectra were simulated and their contributions removed from the experimental spectrum. The residual ^{16}O^{17}O^{1}H and ^{17}O^{17}O^{1}H contributions showed little resolution but distinctive broadening due to strong anisotropic coupling to OH. The low- and high-field features place constraints on the parameters as did the average coupling constants derived from the solution spectra. Iteration involving all four isotopomers followed. The most satisfactory results (Table I, Figure 5) indicate

(31) Corbin, J. L.; Miller, K. F.; Pariyadath, N.; Wherland, S.; Bruce, A. E.; Stiefel, E. I. *Inorg. Chim. Acta* **1984**, *90*, 41.
(32) Miller, R. F.; Wentworth, R. A. D. *Inorg. Chem.* **1980**, *19*, 1818.
(33) Wedd, A. G.; Spence, J. T. *Pure Appl. Chem.* **1990**, *62*, 1055.
(34) The isotropic liquid solution spectrum could be simulated assuming this level of enrichment (cf. Figure 2 of ref 9). The decrease from the expected level of >50 atom % ^{17}O must be due to exchange with $^{16}OH_2$ in the solvents.
(35) Bray, R. C. *JIB* **1979**, *11*, 355.

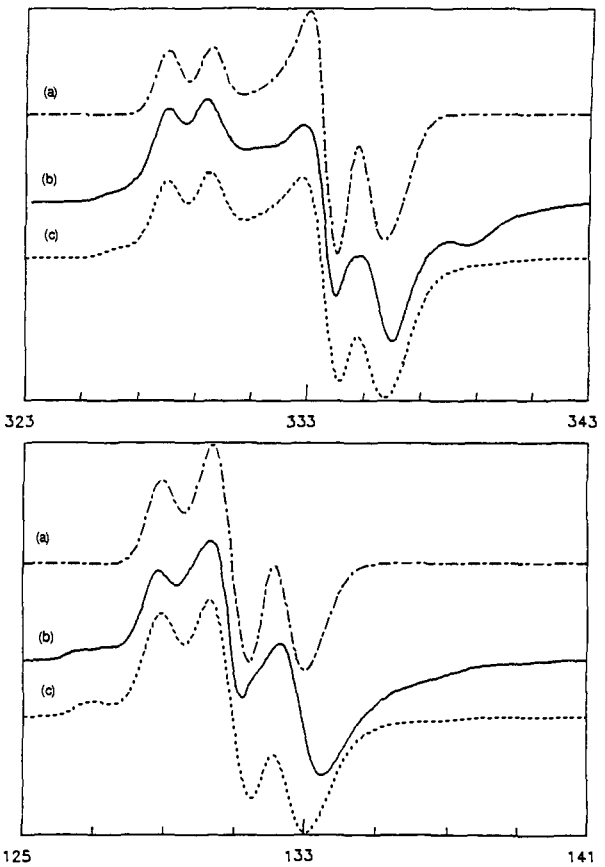

Figure 5. Experimental and simulated spectra of [MoO(OH)L] (^{98}Mo, I = 0, 98.75 atom %) in 1:1 thf:MeCN, $Bu^n_4BF_4$ (0.1 M), and H_2O (2 M); 130 K: (a) ^{16}O, I = 0, 100 atom %; (b) ^{17}O, I = $^5/_2$, 40 atom %; (c) simulation of (b).

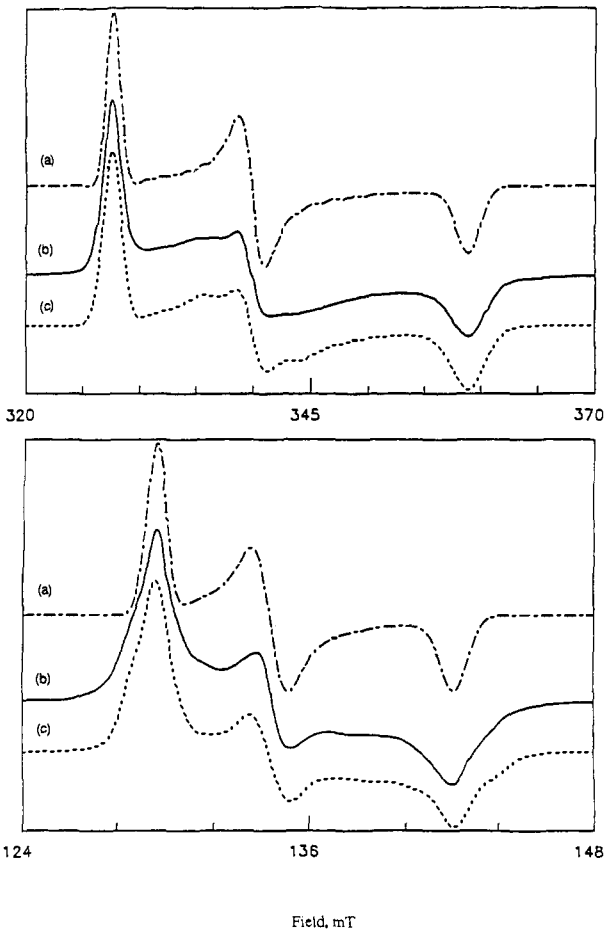

Figure 6. Experimental and simulated spectra of $[MoO_2L]^-$ (^{98}Mo, I = 0, 98.75 atom %) in 1:1 thf:MeCN, $Bu^n_4BF_4$ (0.1 M), and H_2O (2 M); 130 K: (a) ^{16}O, I = 0, 100 atom %; (b) ^{17}O, I = $^5/_2$, 50 atom %; (c) simulation of (b).

that the strongest OH coupling is in the x direction. Its association with this feature is confirmed by its link to the strongest ^1H coupling component, also associated with the x direction.[15]

$[MoO_2L]^-$. All features are broadened by ^{17}O coupling (Figure 6) and some structure is apparent in one or more of the anisotropic components at both 9.1 and 3.6 GHz. The spectrum of $[Mo^{16}O_2L]^-$ has been simulated successfully assuming C_{2v} local symmetry (Figure 7),[15] implying the presence of two equivalent oxo ligands. For the present simulation, the contribution due to the $^{16}O_2$ isotopomer was removed initially. The derived A(^{17}O) (Table I) provides an excellent simulation at both frequencies (Figure 6).

Discussion

Analog Compounds. The tensors **g** and A(^{95}Mo) for [MoO(SH)L] are essentially axial.[15] The present work shows that A(^{17}O) is also axial and of similar magnitude and anisotropy to that seen previously in $[MoO(SPh)_4]^-$ (Table I).[27a] The average coupling of 2.2×10^{-4} cm^{-1} is small. This is consistent with the magnetic orbital d_{xy} being orthogonal to all oxo valence orbitals in an isolated $[Mo^VO]^{3+}$ fragment.[36] A(^{17}O) coupling is weakest (0.75×10^{-4} cm^{-1}) in the z direction, again suggesting an unfavorable direct interaction with the MoO bond. Coupling in the other two components is 3×10^{-4} cm^{-1}, consistent with a dipolar interaction dominating.

Previous work[15] showed that the oxo ligand dominates the ligand field in $[Mo^VOSL]^-$ and that A(^{95}Mo) is very similar in magnitude and anisotropy to that of [MoO(SH)L]. This similarity extends to A(^{17}O) where the average interaction is the same in both species (Table I). However, A(^{17}O) is rhombic in $[Mo^VOSL]^-$ (Table I), consistent with the extensive delocalization of unpaired electron spin onto the thio ligand detected via ^{33}S coupling.[15] Again coupling in the z direction appears to be weaker.

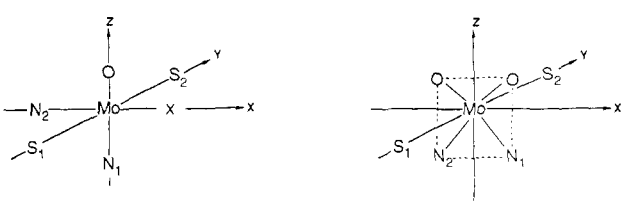

Figure 7. Coordinate systems for (a) MoOXL (X = OH, SH, S) and (b) $[MoO_2L]^-$.

Coupling to the two inequivalent O atoms in [MoO(OH)L] is observed unambiguously in liquid solution at −42 °C. The uncertainties associated with the two A(^{17}O) derived from frozen solution (Table I) are large. However, the magnitude and anisotropy associated with the more weakly coupled oxygen allows assignment to an oxo ligand in an environment very similar to those discussed above. Then, coupling to the hydroxo oxygen is seen to be larger in magnitude and rhombic, with the largest component in the x direction. A more detailed interpretation is not justified with the present data.

The highly characteristic **g** and A(^{95}Mo) for $[MoO_2L]^-$ were derived assuming C_{2v} local symmetry and equivalent oxo ligands (Figure 7b).[15] A(^{17}O) is also characteristic. The average value of $7.7(3) \times 10^{-4}$ cm^{-1} is, coincidently, close to that for the hydroxo oxygen of [MoO(OH)L], but the anisotropy is dramatically different with the strongest component being along the y direction. This is consistent with a strong 3-center π interaction between the two O(p_y) orbitals and Mo(d_{xy}) (Figure 7b). The latter was previously proposed to be the magnetic orbital.[15] The usual

(36) Gray, H. B.; Hare, C. R. *Inorg. Chem.* **1962**, *1*, 363.

Scheme I

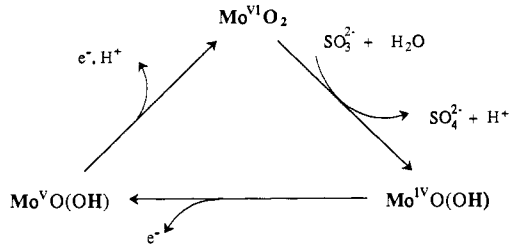

simplistic assumptions[37] suggest a spin density of about 0.1 electron on each oxo ligand. This strong and anisotropic interaction is similar in concept but different in detail to that observed for the ^{33}S thio ligand in $[MoOSL]^-$.[15] In the latter species, a strong 2-center π interaction between $Mo(d_{xy})$ and $S(p_y)$ is responsible (Figure 7a) with the oxo ligand formally orthogonal to the magnetic orbital at this level of treatment.

Comparison of Xanthine Oxidase and Analog Compound Data. The ^{17}O hyperfine signature of the oxo ligand in a $[Mo^VO]$ unit is clear from the analog compound data of Table I: $A_z < A_x, A_y$ with the average value in the range 2.0–2.5 × 10^{-4} cm^{-1}. The formaldehyde inhibited center[12] is the only XnO signal which appears to exhibit such behavior. Assuming that the normal pattern of $g_z > g_x, g_y$ allows proper assignment of A_z (Table I), there would appear to be at least one oxo group present in this inhibited center. The characteristics of the $[Mo^VO_2]$ center seen in $[MoO_2L]^-$ ($g_z < g_x, g_y$; $A_y > A_x, A_z$) are definitely absent, however, suggesting that the second oxygen atom is associated with the inhibiting ligand generated from formaldehyde.

The average value of 12.6 × 10^{-4} cm^{-1} observed for the Very Rapid signal is greater than those seen for the Rapid Type 1, Rapid Type 2, and Slow signals which fall in the range 5–9 × 10^{-4} cm^{-1}. Appeal to the anisotropic parameters reveals very different patterns of behavior.

The OH oxygen in [MoO(OH)L] and the Rapid Type 1 center have similar characteristics: $g_z > g_x, g_y$; $A_x > A_y, A_z$ (Table I). The Rapid Type 1 signal has been assigned previously to a $[Mo^VO(SH)(OR)]$ center (OR, bound product) on the basis of **g**, $A(^{95}Mo)$, $A(^1H)$, and $A(^{33}S)$ data, coupled with chemical considerations.[15] The probability of it being a $[Mo^VO(SH)(OH)]$ center must now be entertained. No direct evidence via ^{17}O coupling for the oxo ligand can be detected: it reveals its presence in the characteristic **g** and $A(^{95}Mo)$ principal values observed in $[Mo^VO]$ species.[15,28a]

There is uncertainty in the assignment of A_x and A_y in the borate Rapid Type 2 signal. Given that **g** is nearly axial, this in no way affects assignment of the highly anisotropic ^{17}O coupling to an OH ligand via comparison with [MoO(OH)L]. Consequently, the assignment[4,15] of the Rapid Type 2 signal as a $[Mo^VO(SH)(OH)]$ center is strengthened.

g, $A(^{95}Mo)$, $A(^{33}S)$, and now $A(^{17}O)$ observed for the Rapid Type 1 and 2 signals are very similar.[15] However, $A(^1H)$ are strikingly different. While coupling to two hydrogens is seen in both signals, both are strongly coupled in Rapid Type 2 (av, 14.0, 10.6 × 10^{-4} cm^{-1}) but one is weakly coupled in Rapid Type 1 (av, 12.5, 2.8 × 10^{-4} cm^{-1}).[4] If both signals arise from $[Mo^VO(SH)(OH)]$ centers, the origin of such differences must be addressed (*vide infra*).

The Very Rapid signal has been assigned to a $[Mo^VOS(OR)]$ center on the basis of coupling to ^{33}S (highly characteristic of $[Mo^VOS]$)[15] and to ^{13}C (consistent with coupling to the OC_8 fragment of bound uric acid product OR),[12b] as well as its relationship to the alloxanthine inhibited signal. The latter exhibits **g** and $A(^{33}S)$ closely related to those of the Very Rapid signal. It also exhibits ^{14}N coupling, assigned to bound inhibiting

Scheme II

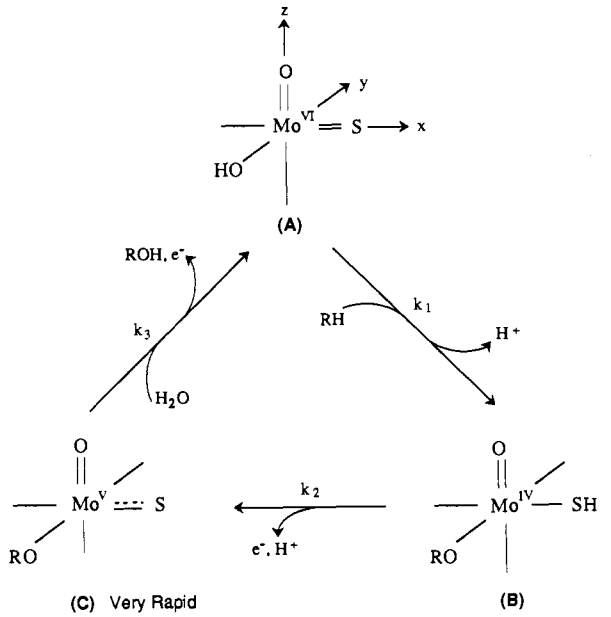

substrate, but no ^{17}O coupling.[38] Alloxanthine features an N_8 atom substituted for the C_8 atom of xanthine or uric acid.

The coupling observed to a single ^{17}O atom in the Very Rapid signal is very different from that seen in the other signals in that it is both strong and isotropic (Table I).[29] Similar behavior is not seen in the oxo and hydroxo ligands of any of the present analog complexes (Table I). A model of a $[Mo^VOS(OR)]$ center does not exist to test the assignment to an OR ligand (structure I). In the enzyme, the electronically delocalized natures of the $[Mo^VOS]$ fragment,[15] the probable dithiolene ligand associated with the pterin cofactor,[11] and the purine substituent of the OR group combine to make prediction difficult. Again, the "silence" of the oxo ligand in terms of its ^{17}O coupling is noteworthy. Nevertheless, on balance, the case for assignment of the Very Rapid signal to a $[Mo^VOS(OR)]$ center remains compelling.

Mechanism of Reaction. A generalized oxygen atom transfer mechanism has been suggested[5,22] for the molybdenum enzymes. A specific example, sulfite oxidase, features a *cis*-$[Mo^{VI}O_2]$ resting state, and the two-electron oxidation of substrate sulfite to sulfate is interpreted[5,39] in terms of the minimal catalytic cycle of Scheme I. Note that transfer of an oxo ligand and its replacement from H_2O occurs in the Mo^{VI} to Mo^{IV} transformation and that at least one oxo ligand is present at each stage. The transient existance of a $Mo^{IV}O(OR)$ (OR = OSO_3) intermediate is implied and is consistent with the known kinetic, EPR, and EXAFS properties[39–41] of sulfite oxidase. It is supported by an analog system[42] which reproduces the essential features of Scheme I. The state of protonation at the Mo^{IV} level is not known: an OH_2 or an OH ligand may be present.

An oxygen atom transfer mechanism equivalent to that of Scheme I can be derived for xanthine oxidase utilizing a $[Mo^{VI}OS]$ resting state and $[Mo^{IV,V}O(SH)]$ intermediates. The transient existence of a deoxomolybdenum(IV) species is implied, prior to replacement of oxo ligand from H_2O. The time resolution of existing physical data has not allowed detection of such a center, and all of the available information is consistent with the presence of a molybdenum–oxo linkage at each stage. While a deoxo intermediate cannot be precluded, the present work shows that there is no need to postulate its existance.

(37) Goodman, B. A.; Raynor, J. B. *Adv. Inorg. Chem. Radiochem.* **1970**, *13*, 135.

(38) Hawkes, T. R.; George, G. N.; Bray, R. C. *Biochem. J.* **1984**, *218*, 961.

(39) Rajagopalan, K. V. *Biochem. Elem.* **1984**, *3*, 149.

(40) Gutteridge, S.; Lamy, M. T.; Bray, R. C. *Biochem. J.* **1980**, *191*, 285.

(41) Cramer, S. P.; Gray, H. B.; Rajagopalan, K. V. *J. Am. Chem. Soc.* **1978**, *100*, 2772.

(42) Xiao, Z.; Young, C. G.; Enemark, J. H.; Wedd, A. G. *J. Am. Chem. Soc.* **1992**, *114*, 9194.

Scheme III

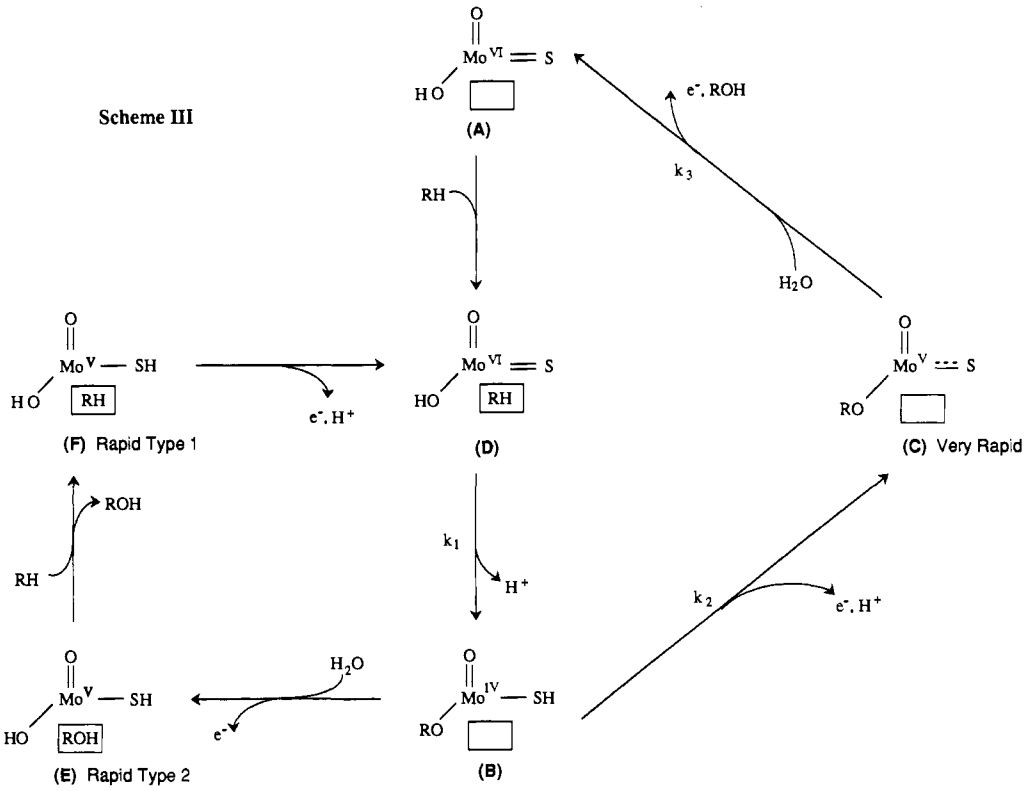

The new ^{17}O coupling information augments **g**, **A**(^{95}Mo), **A**(^{1}H), **A**(^{33}S), and **A**(^{13}C) data discussed previously[15] and suggests that the following centers are responsible for the characteristic xanthine oxidase EPR signals:

Very Rapid:	$[Mo^{V}OS(OR)]$
Rapid Type 1:	$[Mo^{V}O(SH)(OH)]$
Rapid Type 2:	$[Mo^{V}O(SH)(OH)]$
Slow:	$[Mo^{V}O(OH)]$

The Mo^{V} centers derived from the active resting form $[Mo^{VI}OS]$ involve *three* defined ligands. Formulation of that resting form as *fac*-$[Mo^{VI}OS(OH)]$, species A, allows the minimal catalytic cycle of Scheme II to be derived (the rate constants k_{1-3} are those defined by Hille[18]). Note the following: (i) the *cis*-$[Mo^{VI}O(OH)]$ fragment in A is the equivalent of $[Mo^{VI}O_2]$ present in sulfite oxidase and spectator metal–oxo bonds have been proposed to play central roles in olefin metathesis and in allylic rearrangements;[43-45] and (ii) the thio ligand maintains its suggested role as a strongly basic center needed to activate the C_8H bond of xanthine.[15]

The metal valence d orbitals directly involved in the catalysis are of π symmetry: xy, yz, xz. The complete misalignment of **g** and **A**(^{95}Mo) in the Very Rapid signal[13] indicates that center C is of low point symmetry, C_1 or C_i, and that the π-based molecular orbitals will be extensively mixed.

Experimental ^{33}S coupling data show that the oxo ligand dominates the bonding via a Mo–oxo multiple bond with Mo(xz, yz)–O(x, y) π components (Figure 7a; Scheme IIC). The Mo–thio link features a Mo(xy)–S(y) π component, but the formal bond order is 1.5 due to occupation of the antibonding partner, $MoS\pi^*$, by the magnetic electron. The formal MoS bond order of two is restored upon oxidation to resting species A via electron transfer to the internal electron transfer chain. Substrate oxidation is initiated by a concerted interaction of the C_8H bond of xanthine with the *cis*-$[Mo^{VI}S(OH)]$ fragment of A in the xy plane. This leads to formation of the Mo–OR link, population of the Mo(xy)–S(y)π^* orbital, and protonation of the thio ligand, as seen in species B in Scheme II.

The discussion so far is consistent with the behavior of xanthine oxidase under substrate-limiting conditions.[18] Further rationalization of the detailed properties of xanthine oxidase is possible after discussion of three additional points: (i) The first is the presence in the resting form of a $[Mo^{VI}OS]^{2+}$ center. For coordination numbers above four, such centers are highly reactive due to the conjugation of oxidizing Mo^{VI} and reducing thio components and have long been a major synthetic challenge. Young[46] has now shown that the complex $\{HB(Me_2pz)_3\}MoOS(\eta^1\text{-}SP(S)Pr^i_2)$ features a *cis*-$[Mo^{VI}OS]^{2+}$ unit stabilized by a weak interaction between the thio ligand and the "noncoordinated" sulfur atom of the η^1-dithiophosphate via the LUMO $MoS\pi^*$. It is possible that the analogous center in xanthine oxidase may be stabilized similarly by interaction with a cysteinyl or molybdopterin sulfur atom or with a base of similar properties. The interaction would be severed upon initiation of catalysis and protonation of the thio ligand. (ii) There is an "anion-binding site" in xanthine oxidase[21] which is now assigned to the OH ligand position in species A. (iii) There is kinetic evidence that both substrate binding to and product dissociation from the *reduced* enzyme are two-step processes.[19,47,48] One interpretation is that initial substrate binding is non-covalent and catalysis leads to occupation of the anion-binding site by bound product OR, as in species B (Scheme II). Product dissociation follows a reverse sequence.

Scheme III outlines a detailed molecular mechanism of reaction: (i) Substrate is bound non-covalently (as indicated by the box) to form the Michaelis complex D and initiation of catalysis leads to the Mo^{IV} center B.[9,49] (ii) Under substrate limiting conditions, the catalytic cycle is completed via C (Very Rapid),

(43) Rappe, A. K.; Goddard, W. A., III *Nature* **1980**, *285*, 311.
(44) Rappe, A. K.; Goddard, W. A., III *J. Am. Chem. Soc.* **1982**, *104*, 448.
(45) Belgacem, J.; Kress, J.; Osborn, J. A. *J. Am. Chem. Soc.* **1992**, *114*, 1501.
(46) Eagle, A. A.; Laughlin, L. J.; Young, C. G.; Tiekink, E. R. T. *J. Am. Chem. Soc.* **1992**, *114*, 9195.
(47) Hille, R.; Stewart, R. C. *J. Biol. Chem.* **1984**, *259*, 1570.
(48) Davis, M. D.; Olson, J. S.; Palmer, G. *J. Biol. Chem.* **1984**, *259*, 3526.
(49) Oertling, W. A.; Hille, R. *J. Biol. Chem.* **1990**, *265*, 17446.

as in minimal Scheme II. (iii) The Very Rapid EPR signal of xanthine oxidase appears ($t_{1/2}$, 10 ms) under substrate limiting conditions and is accompanied or replaced by the Rapid signal ($t_{1/2}$, 25 ms) with excess xanthine present. Under the latter conditions, an alternative route is available via E (Rapid Type 2) and F (Rapid Type 1). (iv) Species E is proposed to be the [$Mo^{V}O(SH)(OH)$] center responsible for the Rapid Type 2 signal and features non-covalently bound product and two "strongly coupled" protons. It is not seen during normal enzymatic turnover but can be stabilized by interaction of reduced enzyme with product uric acid or with borate.[21,25] (v) The transformation of E to F generates the Rapid Type 1 signal. The position in the catalytic cycle is consistent with the observation that the source of the strongly coupled proton is the C_8H group of a *prior* substrate reaction.[21] The inequivalent hyperfine coupling to the two protons is assigned to differential interaction with substrate RH or with basic amino acid side chains. (vi) Consistent with Hille's suggestion,[18] species F is catalytically incompetent until oxidation to D, the Michaelis complex.

The present proposal accommodates a number of other aspects of xanthine oxidase activity including its role as an N-oxide reductase[5,50] and the fact that warming the Rapid Type 2 signal (species E) leads to the Very Rapid signal (species C).[51] It is consistent with Bray's original mechanism[19] but not with a more recent revision.[13]

The above proposals assume that the putative bidentate dithiolene ligand provided by the molybdenum cofactor[11] plays no direct role in the reaction mechanism. The fact that three molybdenum ligand positions can be defined in the resting form *fac*-[$Mo^{VI}OS(OH)$] means that five ligand positions in the molybdenum center are now defined.

Acknowledgment. A.G.W. and J.R.P. thank the Australian Research Council for financial support. R. Hille and C. G. Young are thanked for stimulating discussions.

(50) Murray, K. N.; Watson, J. G.; Chaykin, S. *J. Biol. Chem.* **1966**, *241*, 4798.

(51) Bray, R. C.; Barber, M. S.; Lowe, D. J. *Biochem. J.* **1978**, *171*, 653.